The Journal of Experimental Biology 200, 975–988 (1997)
Printed in Great Britain © The Company of Biologists Limited 1997
JEB0665

REACTION–DIFFUSION ANALYSIS OF THE EFFECTS OF TEMPERATURE ON HIGH-ENERGY PHOSPHATE DYNAMICS IN GOLDFISH SKELETAL MUSCLE

MARK J. HUBLEY[1,*], BRUCE R. LOCKE[2] AND TIMOTHY S. MOERLAND[1,†]

[1]*Department of Biological Science, Florida State University, Tallahassee, FL 32306-3050, USA* and
[2]*Department of Chemical Engineering, FAMU-FSU College of Engineering, Tallahassee, FL 32310-6046, USA*

Accepted 14 January 1997

Summary

Thermal acclimation results in dramatic changes in the fractional volume of mitochondria within skeletal muscle of teleost fish. We investigated the hypothesis that changes in mitochondrial volume represent a compensatory response to temperature-induced changes in intracellular diffusion coefficients (*D*) of the high-energy phosphate compounds ATP and creatine phosphate (PCr). Using ^{31}P nuclear magnetic resonance spectroscopy, we determined D_{PCr} and D_{ATP} in goldfish (*Carassius auratus*) skeletal muscle at 25 °C and 5 °C: D_{PCr} was $3.28\pm0.18\times10^{-6}$ cm^2 s^{-1} at 25 °C and $2.00\pm0.09\times10^{-6}$ cm^2 s^{-1} at 5 °C; D_{ATP} was $2.13\pm0.16\times10^{-6}$ cm^2 s^{-1} at 25 °C and was estimated to be 1.30×10^{-6} cm^2 s^{-1} at 5 °C. There was no evidence for an effect of acclimation temperature or fiber type on D_{ATP} or D_{PCr}. A mathematical reaction–diffusion model was used to calculate profiles of [ATP], [PCr] and the free energy of ATP hydrolysis (ΔG_{ATP}) in activated goldfish muscle fibers at 5 °C and 25 °C. The results showed spatial and temporal constancy of [ATP], [PCr] and ΔG_{ATP} in red fibers at both temperatures, regardless of changes in acclimation temperature or mitochondrial density. The model also showed spatial and temporal constancy of [ATP] in white fibers at 5 °C and 25 °C, but gradients in [PCr] and ΔG_{ATP} developed in white fibers under all conditions of temperature and acclimation temperature. These gradients were attenuated in cold-acclimated animals by cold-induced increases in mitochondrial density. However, the model shows that the proximal stimulus for temperature-induced changes in mitochondrial volume density in muscle is not a disruption in intracellular diffusion of high-energy phosphates.

Key words: ATP, goldfish, *Carassius auratus*, creatine phosphate, energetics, nuclear magnetic resonance, thermal acclimation, mitochondrial volume density.

Introduction

Most species of fish are in thermal equilibrium with their environments, so acute or seasonal changes in temperature present these ectotherms with a number of challenges to locomotor performance. Among these are changes in the catalytic rates of enzymes involved in energy metabolism (Hazel and Prosser, 1974) and changes in intracellular diffusion coefficients (*D*) of cytosolic metabolites (Sidell and Hazel, 1987). Despite the effects of temperature on cellular metabolism, many species of fish maintain high levels of biological activity over a broad range of environmental temperatures. Goldfish (*Carassius auratus*), for example, may remain active from near freezing temperatures to above 30 °C, provided they are given time to acclimate to changes in temperature (Johnston *et al*. 1975; Johnson and Bennett, 1995).

Several weeks of acclimation to a new temperature result in various modifications to the ultrastructure of skeletal muscle in teleost fish. Among these modifications are significant changes in the fractional volume of muscle fibers occupied by mitochondria (Sidell, 1988). An inverse correlation between mitochondrial density and acclimation temperature was first observed in carp (*Carassius carassius* L.) (Johnston and Maitland, 1980) and has since been observed in several unrelated species with dissimilar lifestyles and modes of locomotion (Sidell, 1988; Moerland, 1995). Mitochondrial proliferation thus appears to be a widespread response to cold-acclimation among teleosts. The extent of this acclimation-induced change in skeletal muscle ultrastructure may be considerable: twofold or greater increases in mitochondrial density have been observed upon cold-acclimation in red and white fibers from cold-acclimated carp (Johnston, 1982) and goldfish (Tyler and Sidell, 1984).

Two categories of interpretation have been offered regarding the functional significance of temperature-related changes in mitochondrial density. First, an increase in the number of mitochondria at low temperatures, accompanied by an increase in quantity of mitochondrial enzymes, may compensate for

*Present address: Department of Biology, Washington College, Chestertown, MD 21620, USA.
†Author for correspondence (e-mail: moerland@bio.fsu.edu).

reduced catalytic rates of individual mitochondrial enzymes (Johnston and Maitland, 1980; Johnston, 1982; Egginton and Sidell, 1989). According to this interpretation, changes in mitochondrial density help to maintain constant levels of oxidative capacity across a range of temperatures. Second, increased mitochondrial density at low temperatures, which also results in reductions of the mean diffusion path lengths between mitochondria and other cytosolic compartments, may compensate for reduced diffusion coefficients of cytosolic metabolites (Johnston, 1982; Tyler and Sidell, 1984; Sidell, 1988; Egginton and Sidell, 1989). Accordingly, changes in mitochondrial density help to maintain a constant diffusive flux of oxygen between mitochondria and capillaries and a constant diffusive flux of cytosolic metabolites between mitochondria and other cytosolic compartments. Sidell (1988) has predicted that changes in mitochondrial density allow a constant diffusive flux of cytosolic metabolites at temperatures ranging from 5 °C to 25 °C, even if diffusion coefficients at 5 °C are reduced to 29 % of their values at 25 °C.

In this paper, we examine the second category of hypothesis, that acclimatory adjustments in mitochondrial density are a response to temperature-related changes in intracellular diffusion. This hypothesis is examined in the context of two 'high-energy phosphate' compounds, ATP and creatine phosphate (PCr). Intracellular diffusive transport of these compounds is critical for supplying energy to myosin ATPase during muscle contraction (Bessman and Geiger, 1981; Meyer *et al*. 1984). Goldfish were selected as the system for study because acclimation-induced changes in muscle-cell ultrastructure are well documented for this species (Tyler and Sidell, 1984). There were three objectives of this study. (i) To quantify the effects of temperature on intracellular diffusion of ATP and PCr. We used pulsed-field gradient ^{31}P nuclear magnetic resonance spectroscopy (PFG ^{31}P NMR) to determine D_{ATP} and D_{PCr} in goldfish skeletal muscle at 5 °C and 25 °C. (ii) To assess the effects of temperature on the capacity of goldfish to maintain a constant concentration of ATP and free energy of ATP hydrolysis (ΔG_{ATP}) throughout activated muscle fibers. We used a mathematical reaction–diffusion model to analyze spatial variations in the concentrations of high-energy phosphate compounds and ΔG_{ATP} in goldfish muscle fibers at 5 °C and 25 °C. (iii) To assess the functional significance of changes in mitochondrial density on the capacity to maintain constant [ATP] and ΔG_{ATP} throughout activated muscle fibers. We used the reaction–diffusion model to analyze the effects of changes in mitochondrial density on the concentrations of high-energy phosphate compounds and ΔG_{ATP} in goldfish muscle fibers.

Materials and methods

Animals and surgical procedures

Goldfish (*Carassius auratus* L.) were purchased from Pineland Plantation Fish Farm (Newton, GA, USA) and housed in tanks (1000 l) containing biologically filtered, recirculating well water. Fish were acclimated to either 25 °C or 5 °C (±1 °C) for at least 6 weeks prior to experiments. Acclimation for this period results in significant changes in the activities of metabolic enzymes and the proportions of muscle fiber types (Sidell, 1980) and in the volume of muscle fibers occupied by mitochondria (Tyler and Sidell, 1984). Water temperature was regulated with a combination of chiller units (Frigid Units, Inc., Toledo, OH, USA) and immersion heaters (Sethco, Hauppauge, NY, USA). Fish were fed commercial catfish chow and maintained on a 12 h:12 h light:dark cycle. Upon dissection, goldfish acclimated to 25 °C weighed 218±27 g (N=12), and goldfish acclimated to 5 °C weighed 183±35 g (N=12). This difference in mass was not significant (P=0.94, Mann–Whitney rank sum test).

Fish were anesthetized prior to surgery with 100 mg l^{-1} tricaine methanesulfonate. Red muscle fibers were dissected from the lateral line region, and white muscle fibers were dissected from the anterior epaxial region. These preparations consist of uniform populations of red and white fibers, respectively (Johnston and Lucking, 1978). For ^{31}P nuclear magnetic resonance (NMR) spectroscopy, strips of red or white muscle (approximately 2 mm in diameter and 90 mg in mass) were removed from the goldfish and held in ice-cold Ringer's solution (prepared according to the method of Langfeld *et al*. 1991) prior to placement in the NMR probe. For subsequent assays of enzyme activity, additional samples of red and white muscle were stored in liquid nitrogen. Anesthetized animals were killed by severance of the spinal cord and pithing.

^{31}P NMR spectroscopy

Phosphorus NMR was conducted at 109 MHz using a Bruker HX-270 spectrometer and a PFG NMR probe designed for small tissue samples. The NMR hardware and procedures have been described previously (Hubley and Moerland, 1995; Hubley *et al*. 1995). In brief, a strip of red or white muscle was fixed in the NMR sample tube, which was oriented in the x,y-plane relative to the B_0 magnetic field. Isolated tissue was continuously superfused with Ringer's solution, which was maintained at 25 °C or 5 °C (±0.5 °C) and equilibrated with 95 % O_2:5 % CO_2 gas. These tissue preparations were metabolically stable for more than 6 h after dissection (Hubley *et al*. 1995), and experiments were conducted within 6 h. Four PFG NMR spectra (gradient pulse magnitudes 0, 41×10^{-4}, 128×10^{-4} and 195×10^{-4} T cm^{-1}, where 1 T = 10^4 gauss) were acquired from each sample using a homonuclear decoupled spin echo (HDSE) pulse sequence (Hubley and Moerland, 1995). The effective time over which diffusion was monitored was 9.2 ms. The magnetic field gradient was applied along the z-axis, relative to the B_0 magnetic field, and diffusion coefficients were measured perpendicular to the long axes of the muscle fibers. To determine relative metabolite concentrations and confirm metabolic stability of the tissue, we acquired fully relaxed (12 s recycle delay), pulse-acquire ^{31}P NMR spectra before and after each series of diffusion spectra (Fig. 1).

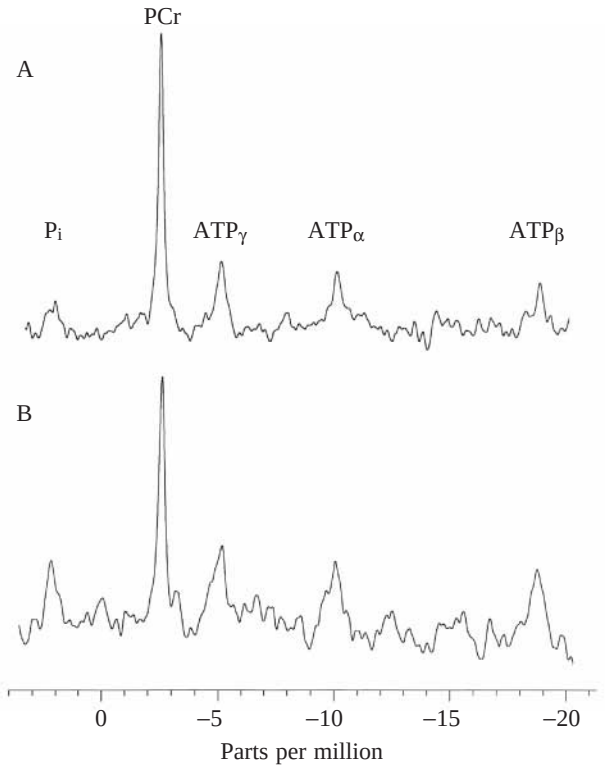

Fig. 1. Representative fully relaxed ^{31}P nuclear magnetic resonance spectra of goldfish skeletal muscle. (A) White muscle; (B) red muscle. Spectra are for tissue from animals acclimated to 25 °C and were obtained at 25 °C. Spectra represent 72 free induction decays acquired using a $\pi/2$ radiofrequency pulse and a 12 s recycle delay. P_i, inorganic phosphate; PCr, phosphocreatine.

Creatine kinase assays and metabolite concentrations

For use in modeling, the maximum velocity (V_{max}) of the creatine kinase (CK) reaction was estimated from spectrophotometric assays of CK activity in crude tissue homogenates. Assays were performed at 5 °C and 25 °C on red and white muscle from goldfish acclimated to either 5 °C or 25 °C. CK activity in the direction of ATP formation was measured according to the method of Lowry and Passonneau (1972); reaction velocities (V) were determined at six different concentrations of PCr (range 1.5–44 mmol l^{-1}). Lineweaver–Burke double reciprocal plots of $1/V$ *versus* 1/[PCr] were used to determine V_{max}. Units of V_{max} were converted to mmol l^{-1} s^{-1}, required by the model, on the assumption that 70 % of the wet tissue mass is intracellular water.

The concentration of ATP and the total concentration of creatine ($[creatine]_{total}$=[creatine]+[PCr]) in red and white muscle were determined using high-performance liquid chromatography (HPLC). Excised muscle tissue was rapidly frozen with freeze clamps, perchloric acid extracts of the tissue were prepared as described by Wiseman *et al*. (1992), and HPLC was conducted on a reversed-phase OSD-AQ column (YMC, Inc., Morris Plains, NJ, USA). Absorbance of the eluted metabolites was monitored at 260 nm for ATP and 210 nm for PCr and creatine. Integrated peak areas of ATP, PCr and creatine were converted to metabolite concentrations by comparison with standards. These determinations were performed on tissue from goldfish acclimated to 20 °C, and it was assumed that the concentrations of these metabolites did not vary with an animal's thermal history. This assumption is supported by the observation that [ATP] in red and white muscle of brook trout (*Salvelinus fontinalis*) is not significantly affected by acclimation temperature (Walesby and Johnston, 1980).

We calculated concentrations of PCr and inorganic phosphate (P_i) in red and white muscle by multiplying the HPLC-derived [ATP] by the NMR-derived [PCr]/[ATP] and $[P_i]$/[ATP] ratios (van Waarde *et al*. 1990). These ratios were determined by manual integration of peak areas from fully relaxed ^{31}P NMR spectra. The concentration of creatine was determined by subtraction of [PCr] from the HPLC-derived $[creatine]_{total}$. The concentration of free ADP ($[ADP]_f$) was determined from [ATP], [PCr] and [creatine] on the assumption of equilibrium of the CK reaction (van Waarde *et al*. 1990). Values of parameters determined by NMR (i.e. [PCr]/[ATP] and $[P_i]$/[ATP]) were obtained from fish acclimated to 5 °C and 25 °C.

Mathematical modeling

Diffusion and reaction of compounds involved in energy transport (ATP, free ADP, PCr and creatine) were modeled in a one-dimensional system. This system was defined to extend from the surface of a mitochondrion to a distance equal to half of the mean free spacing between clusters of mitochondria ($\lambda/2$). The parameter $\lambda/2$ approximates the greatest distance between a given point in the cell and a mitochondrion. Values of $\lambda/2$ were derived from the mean free spacing between clusters of mitochondria (λ_a cluster) in goldfish skeletal muscle (Tyler and Sidell, 1984). Reactions catalyzed by CK and myosin ATPase, as well as glycolytic ATP production in white muscle, were assumed to occur homogeneously throughout the domain $0 \leqslant x \leqslant \lambda/2$.

Red and white muscle fibers were analyzed under five conditions of acclimation temperature and experimental temperature: (i) animals acclimated to 25 °C were modeled at 25 °C (25acc–25exp); (ii) animals acclimated to 25 °C were modeled at 5 °C (25acc–5exp), representing an acute decrease in temperature; (iii) animals acclimated to 5 °C were modeled at 5 °C (5acc–5exp); (iv) animals acclimated to 5 °C were modeled at 25 °C (5acc–25exp), representing an acute increase in temperature; and (v) red and white fibers were analyzed under the 5acc–5exp condition with the exception that mitochondrial spacing, $\lambda/2$, was that of fish acclimated to 25 °C. The fifth condition (5acc*–5exp) allowed us to examine the hypothetical situation in which cold-acclimation does not lead to proliferation of mitochondria.

Temporally and spatially dependent concentration profiles of ATP, free ADP, PCr and creatine were calculated according to the following molar-species continuity equation (Bird *et al*. 1960):

$$\frac{\partial C_i}{\partial t} = D_i \frac{\partial^2 C_i}{\partial x^2} + R_i , \qquad (1)$$

where C_i is the molar concentration of species i and t is time. The total rate of reaction, R_i, is equal to the sum of the rates of the CK, myosin ATPase and glycolysis reactions. Calculations were made using the IMSL Fortran subroutine MOLCH (IMSL, Inc., Houston, TX, USA), which uses the method of lines with cubic Hermite polynomials. The following two boundary conditions were applied. (i) $C_i=C_i^o$ at $x=0$, where C_i^o is the resting concentration of species i. Thus, the concentration of each species remains constant at the mitochondrial boundary. This condition implicitly assumes that a mitochondrion has the capacity to buffer perfectly against changes in C_i at its boundary under all conditions and that the regulatory set point of mitochondrial function does not differ with temperature or acclimation state. (ii) $dC_i/dx=0$ at $x=\lambda/2$; this condition provides symmetry about the boundary $x=\lambda/2$. The initial condition was $C_i=C_i^o$ throughout the domain $0\leqslant x\leqslant\lambda/2$ at $t=0$. Values of D used in the model are given in Table 1, reaction parameters are given in the text and in Table 2, and resting metabolite concentrations are given in Table 3.

In a swimming fish, muscle fibers at a given location along the trunk may be activated for approximately 35–50 % of the tailbeat cycle (Jayne and Lauder, 1993, 1995). To mimic the metabolic effects of swimming, our model was run as a series of loops. Each loop lasted for half of the tailbeat cycle, the duration of each loop was dictated by the tailbeat frequency, and the myosin ATPase was activated only during odd-numbered loops. This protocol simulated a 50 % duty cycle for the modeled muscle fibers. In carp, which are phyletically and morphologically similar to goldfish, the transition between sustained swimming (powered exclusively by red fibers) and activation of white fibers occurs at a tailbeat frequency of 3–4 Hz (Rome *et al*. 1984). We analyzed red muscle with tailbeat frequencies of 1 Hz and 4 Hz, and we analyzed white muscle with tailbeat frequencies of 4 Hz, 8 Hz and 12 Hz. The model was run for a number of successive loops corresponding to a total time of 20 s of maximal activity. By definition, sustained swimming can be expected to occur for much longer periods. In our model, however, red fiber concentration profiles had reached steady states within a few seconds. White muscle is progressively recruited as speeds increase above the limit for sustained swimming. The upper limit of locomotory performance, burst speed swimming, is operationally defined as the maximum swimming speed that can be maintained for less than 15 s (Sidell and Moerland, 1989). Results from the model thus reflect both the steady-state profiles resulting from sustained swimming in red muscle and the consequences of burst activity in white muscle.

The kinetic mechanism for CK at neutral pH is a rapid-equilibrium random mechanism in the direction of ATP production and an equilibrium-ordered mechanism in the reverse direction (Schimerlik and Cleland, 1973). Because $[PCr]\gg[ADP]_f$, an equilibrium-ordered mechanism, in which PCr binds before ADP, was assumed for the forward reaction. Accordingly, we used the following approximate expression (derived from Segel, 1993) for the rate of the CK reaction:

$$R_{ATP}^{CK} = \frac{V_{max}}{K_{ib}K_mK_{eq}}\,(C_{PCr}C_{ADP}K_{eq} - C_{ATP}C_{creatine})\,, \quad (2)$$

where K_{ib} is the dissociation constant for PCr and CK, K_m is the apparent Michaelis constant for ADP, K_{eq} is the equilibrium constant, and $R_{ATP}^{CK}=-R_{ADP}^{CK}=-R_{PCr}^{CK}=R_{creatine}^{CK}$. Values of K_{ib} and K_m were taken from the results of Watts (1973) for CK from rabbit muscle; the temperature-dependencies of these parameters were not given. Values of K_{eq} at 5 °C and 25 °C were taken from the results of Teague and Dobson (1992) for rabbit skeletal muscle. The effects of the sources of these and other parameters on the model are addressed in the Results. Values of V_{max} were determined in the present study.

Myosin ATPase was modeled using Michaelis–Menten kinetics (Pate and Cooke, 1985):

$$R_{ATP}^{myo} = \frac{-V_{max}C_{ATP}}{K_m + C_{ATP}}\,, \quad (3)$$

where K_m is the apparent Michaelis constant for ATP and $R_{ATP}^{myo}=-R_{ADP}^{myo}$. Values of V_{max} at 15 °C for red and white skeletal muscle from goldfish acclimated to 5 °C and 25 °C were taken from Sidell (1980). These values were adjusted to V_{max} at 5 °C and 25 °C according to the Arrhenius equation:

$$k = Ae^{-E_a/\boldsymbol{R}T}, \quad (4)$$

where k is equal to V_{max}, A is the pre-exponential factor, E_a is the Arrhenius activation energy, T is absolute temperature and $\boldsymbol{R}$ is the gas constant. Values of E_a for myosin ATPase in goldfish white muscle were taken from the results of Johnston (1979) and are used for both red and white muscle; activation energies were not given for goldfish red muscle. The K_m for myosin ATPase of 150 μmol l^{-1} was obtained from the data of Cooke and Pate (1985) for rabbit psoas muscle.

An estimate of ATP production *via* anaerobic glycolysis was included for white muscle. Anaerobic glycolysis was not included in the analysis of red muscle, because sustained swimming is predominantly supported by aerobic metabolism (Sidell and Moerland, 1989). For simplicity, glycolytic ATP production was modeled as a single, ADP-activated process that obeyed Michaelis–Menten kinetics:

$$R_{ATP}^{gly} = \frac{V_{max}C_{ADP}}{K_m + C_{ADP}}\,, \quad (5)$$

where $R_{ATP}^{gly}=-R_{ADP}^{gly}$. Values of V_{max} were estimated from ATP turnover supported by anaerobic glycolysis during burst activity in trout white muscle (Dobson *et al*. 1987). These values were adjusted to 5 °C and 25 °C with a Q_{10} of 2.7, which is within the range of Q_{10} values measured for glycolytic enzymes from temperate-zone fishes (Crockett and Sidell, 1990). We selected an effective 'K_m' of 50 μmol l^{-1}, so that a substantial rise in the concentration of free [ADP] would result in a rate of glycolysis near V_{max}.

The following equation was used to calculate profiles of ΔG_{ATP} in goldfish skeletal muscle:

$$\Delta G_{ATP} = \Delta G^{\circ}_{ATP} - \boldsymbol{R}T\ln \frac{C_{ADP}}{C_{ATP}C_{P_i}}\ , \quad (6)$$

where ΔG^{o}_{ATP} is the standard free energy of ATP hydrolysis calculated for 5 °C or 25 °C (Krab and van Wezel, 1992). The concentration of P_i was estimated as:

$$C_{Pi} = C^{o}_{Pi} + \Delta C_{creatine} + \Delta C_{ADP}\,, \quad (7)$$

where C^{o}_{Pi} is the resting concentration of P_i. Use of equation 7 requires the following two assumptions: (i) that depletion of PCr results in stoichiometric production of creatine and P_i, and (ii) that net depletion of ATP results in stoichiometric production of ADP and P_i (Kushmerick, 1985).

Statistics

Statistical analyses were performed using SigmaStat (Jandel Scientific Software, San Rafael, CA, USA). Comparisons of population means were made by analysis of variance (ANOVA) or *t*-test when the populations being compared were normally distributed and had equal variance. When either of these criteria was not met, a non-parametric analysis was used as indicated. A significance level of $P<0.05$ was used for all tests. All values are given as the mean ± S.E.M. (N), where N represents the number of independent repetitions performed on samples from different animals.

Results

Diffusion coefficients

Acclimation temperature and fiber type had no significant effects on either D_{ATP} or D_{PCr}. Diffusion coefficients of ATP and PCr in goldfish skeletal muscle were pooled for a given experimental temperature, and these values are shown in Table 1. Direct measurements of D_{PCr} in goldfish skeletal muscle show a significant effect of temperature (Q_{10}=1.28) between 5 °C and 25 °C. Signal-to-noise ratios sufficient to determine D_{ATP} at 5 °C were not obtained with PFG NMR. We attribute the reduction in the ATP signal at 5 °C to a decrease in the ATP transverse relaxation time (T_2), which limits signal in spin echo experiments. For use in the reaction–diffusion analysis, we estimated D_{ATP} at 5 °C from D_{ATP} at 25 °C with the assumption that the Q_{10} for D_{ATP} is equal to that for D_{PCr}.

Table 1. *Intracellular diffusion coefficients of ATP and phosphocreatine*

	$10^6 \times D$ ($cm^2\,s^{-1}$)	
T (°C)	ATP	Phosphocreatine
5	1.30†	2.00±0.09 (24)*
25	2.13±0.16 (15)‡	3.28±0.18 (24)‡

Values are means ± S.E.M. (N).

*Significantly different from the value at 25 °C; $P<0.05$. No significant differences were found between animals held at different acclimation temperatures or between different fiber types. These values were pooled for the given experimental temperature.

†Derived from D_{ATP} (25 °C) as described in the text.

‡Data reported by Hubley and Moerland, 1995.

CK activity and metabolite concentrations

Estimates of V_{max} for CK from goldfish skeletal muscle are shown in Table 2. Temperature acclimation did not have a significant effect on CK maximal activity. Experimental temperature, however, did have a significant effect on CK activity: the pooled Q_{10} was 2.8 between 5 °C and 25 °C. The activity of CK in white muscle was consistently slightly greater

Table 2. *Parameters used in modeling*

		Creatine kinase		Myosin ATPase	Glycolysis
	$\lambda/2$[a] (μm)	V_{max} ($mmol\,l^{-1}\,s^{-1}$)	K_{eq}[b]	V_{max}[c] ($mmol\,l^{-1}\,s^{-1}$)	V_{max}[d] ($mmol\,l^{-1}\,s^{-1}$)
Red muscle					
25acc–25exp[e]	8.90	23.5±4.2	217	3.81	0
25acc–5exp	8.90	3.3±0.7	307	0.30	0
5acc–5exp	2.36	2.3±0.3	307	1.05	0
5acc–25exp	2.36	29.8±4.5	217	4.13	0
White muscle					
25acc–25exp	71.5	30.8±4.5	217	6.92	5.72
25acc–5exp	71.5	4.8±1.0	307	0.54	0.81
5acc–5exp	34.2	5.0±0.5	307	3.52	0.81
5acc–25exp	34.2	31.8±3.3	217	15.20	5.72

Values for creatine kinase V_{max} are means ± S.E.M. (N=6).

Values for each parameter (except creatine kinase V_{max}, which were determined in this study) were derived from data given in the following references: [a]values derived from data given by Tyler and Sidell (1984); [b]values derived from data given by Teague and Dobson (1992); [c]values derived from data given by Sidell (1980); [d]values derived from data given by Dobson *et al.* (1987).

[e]Acclimation conditions, experimental temperatures and abbreviations are defined in Materials and methods.

Table 3. *Metabolite concentrations in goldfish skeletal muscle*

	Red muscle	White muscle
[ATP] (mmol l^{-1})[a]	3.57±0.30 (6)	5.53±0.67 (6)*
[PCr]/[ATP][b]	4.83±0.24 (23)	5.59±0.30 (23)*
[PCr] (mmol l^{-1})[c]	17.2	30.9*
$[Creatine]_{total}$ (mmol l^{-1})[a]	27.8±2.2 (6)	34.5±2.2 (6)
[Creatine] (mmol l^{-1})[d]	10.6	3.6
$[P_i]/[ATP]$[b]	0.90±0.14 (23)	1.06±0.19 (23)
$[P_i]$ (mmol l^{-1})[c]	3.21	5.86*
$[ADP]_f$ (μmol l^{-1})[e]	10	3

Values are means ± S.E.M. (*N*).
*Significantly different from the value for red muscle; $P<0.05$.
[a]Determined using high-performance liquid chromatography.
[b]Determined from fully relaxed ^{31}P NMR spectra.
[c]Calculated by multiplication of the NMR-derived ratio by [ATP].
[d]Calculated by subtraction of [PCr] from $[creatine]_{total}$.
[e]Calculated from the creatine kinase equilibrium.
$[ADP]_f$, free ADP concentration; PCr, phosphocreatine; P_i, inorganic phosphate.

than that of red muscle, but the differences were not statistically significant. Metabolite concentrations for red and white goldfish skeletal muscle are given in Table 3. Differences in acclimation temperature and experimental temperature did not result in significant differences in [PCr]/[ATP] or $[P_i]/[ATP]$. Concentrations of ATP, PCr and P_i in white fibers were significantly greater than those in red fibers, which is consistent with *in vivo* ^{31}P NMR data from goldfish (van den Thillart *et al*. 1990) and with data from extracted tissue of brook trout (Walesby and Johnston, 1980).

Concentration profiles and ΔG_{ATP}

Temporal–spatial profiles of [ATP], [PCr] and ΔG_{ATP}, calculated for maximally activated goldfish red and white skeletal muscle, are shown in Figs 2–6. In Figs 2, 3, 4 and 6, panels A and C show conditions in which acclimation temperature is equal to experimental temperature; panels B and D show profiles resulting from acute changes in temperature. Metabolite concentrations were not substantially affected by changes in tailbeat frequency for times greater than a few tailbeat cycles, and all profiles shown were calculated at 4 Hz.

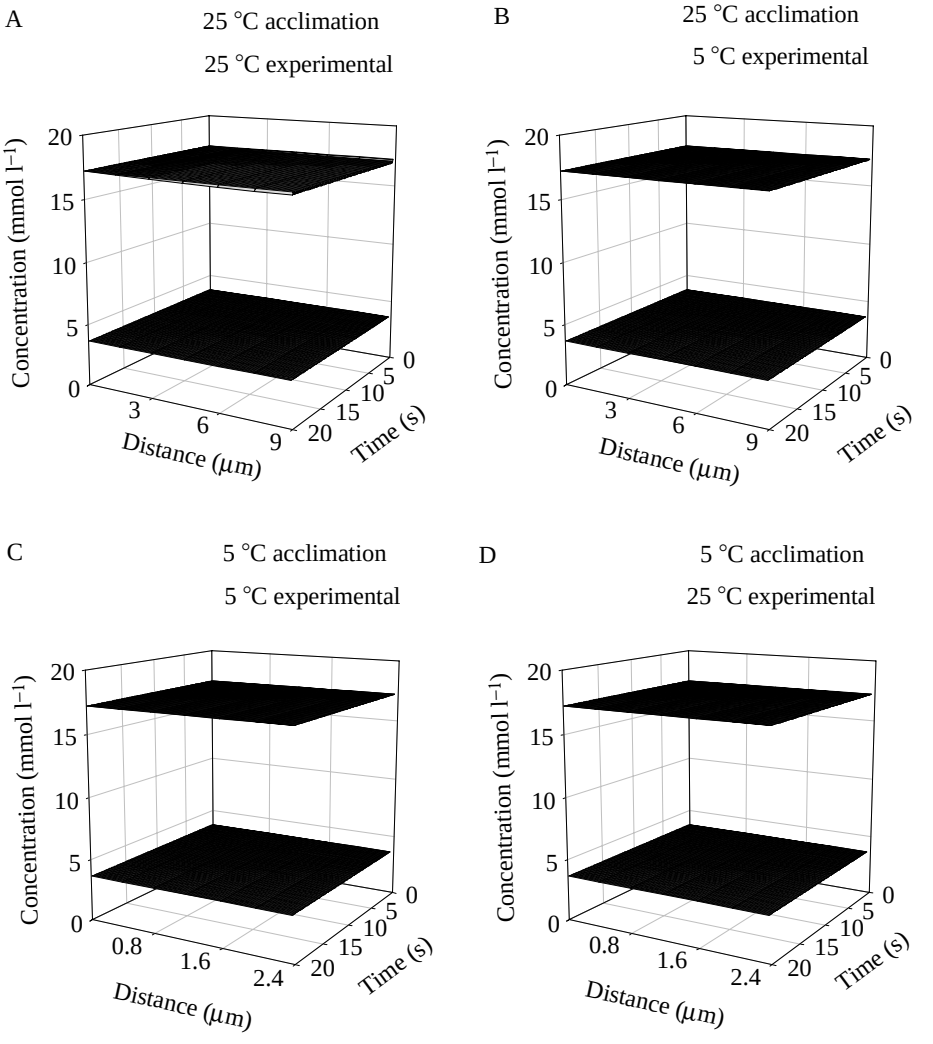

Fig. 2. Concentration profiles of PCr and ATP in activated goldfish red muscle fibers. In each panel, the uppermost curve represents [PCr] and the lowermost [ATP]. Concentration profiles were calculated according to equation 1 as described in the text. 'Distance' in each figure indicates the one-dimensional distance from the surface of a mitochondrion; the maximum distance plotted is half of the mean free spacing between mitochondria, λ/2, which is given in Table 2. 'Time' in each figure indicates the time in seconds after initial activation of the muscle fiber. The tailbeat frequency is 4 Hz.

It may seem intuitive that higher tailbeat frequencies should result in greater depletion of energy, but our model accounts for changes in [ATP] and [PCr] in individual muscle fibers, which are activated in an 'all-or-nothing' manner. Provided that the individual fibers are activated with a given duty cycle for the total duration of activity, the degree of energy depletion in the fibers does not depend on tailbeat frequency.

In red muscle, no changes were observed in [ATP], and changes in [PCr] were less than 2 % (Fig. 2). Similarly, ΔG_{ATP} did not vary by more than 2 % in red muscle (Fig. 3). In white muscle, no substantive changes were observed in [ATP] during 20 s of maximal activity (Fig. 4), but calculations showed the development of marked gradients in [PCr]. Depletion of PCr in white fibers was most extensive at the 25 °C experimental temperature: after 20 s under the condition 25acc–25exp, [PCr] at $x=\lambda/2$ was reduced by 15.2 mmol l^{-1}; under the condition 5acc–25exp, [PCr] at $x=\lambda/2$ was reduced by 11.5 mmol l^{-1}. An expanded view of the changes in [PCr] that occur during contraction and relaxation is shown in Fig. 5. Substantial gradients in ΔG_{ATP} also developed in white muscle (Fig. 6): under the condition 25acc–25exp, the absolute value of ΔG_{ATP} at $x=\lambda/2$ was reduced by 9.1 kJ mol^{-1}; under the condition 5acc–25exp, ΔG_{ATP} at $x=\lambda/2$ was reduced by 7.2 kJ mol^{-1}. Changes in ΔG_{ATP} were driven primarily by increases in [ADP] and [P_i], as per equation 6: net decreases in [ATP] were minimal, although they resulted in large proportional increases in [ADP]. For example, the 9.1 kJ mol^{-1} decrease in ΔG_{ATP} observed under the 25acc–25exp condition was the result of a tenfold increase in [ADP] and a fourfold increase in [P_i], but the decrease in [ATP] was less than 0.4 %.

Most parameters for the reaction–diffusion model were derived from studies of goldfish, but it was not feasible to obtain all information from this species. Estimates of K_{ib}, K_m(ADP) and K_{eq} for the CK reaction, K_m(ATP) for myosin ATPase and glycolytic ATP production were derived from systems other than goldfish skeletal muscle. To assess the sensitivity of the reaction–diffusion model to variations in these parameters, the model was run under conditions in which they were increased or decreased tenfold (in the case of glycolytic ATP production, R_i^{gly} was set equal to zero). In red muscle, tenfold changes in K_{ib}, K_m(ADP), K_{eq} and K_m(ATP) resulted in changes of less than 5 % in the temporal–spatial profiles of [ATP] and [PCr]. In white muscle, tenfold changes in K_{ib}, K_m(ADP) (Fig. 7A) and K_m(ATP) (Fig. 7C) resulted in changes of less than 3 % in

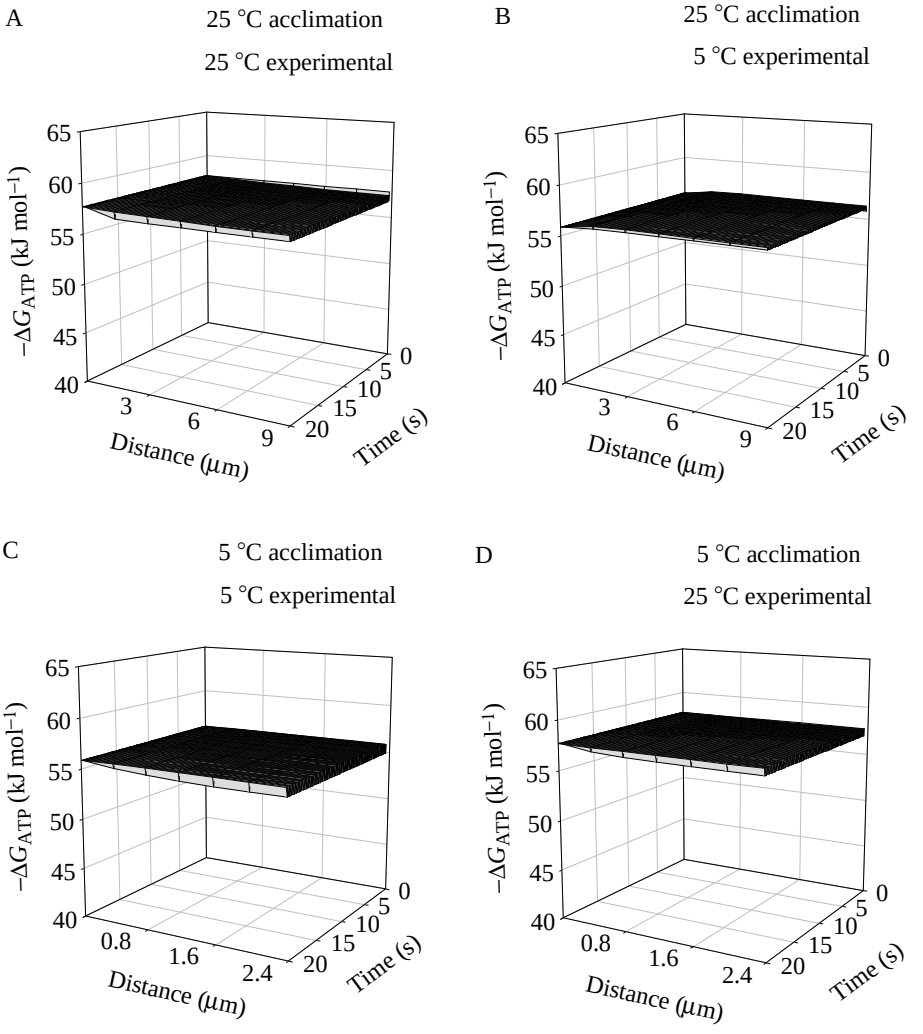

Fig. 3. Profiles of ΔG_{ATP} in activated goldfish red muscle fibers. ΔG_{ATP} was calculated from the concentration profiles of ATP, ADP and P_i according to equation 6.

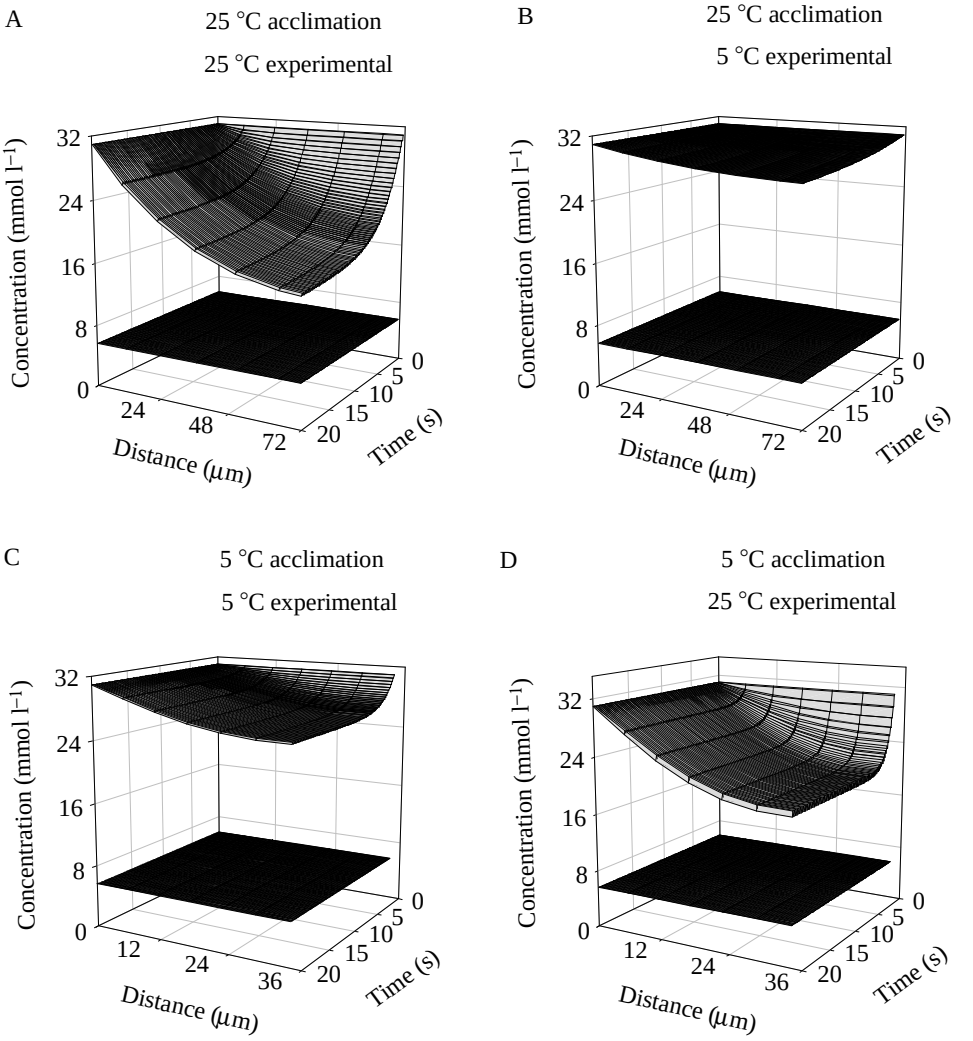

Fig. 4. Concentration profiles of PCr and ATP in activated goldfish white muscle fibers. In each panel, the uppermost curve represents [PCr] and the lowermost [ATP]. For further details, see the legend to Fig. 2.

[ATP] and [PCr]. Tenfold changes in K_{eq} and the removal of glycolytic ATP production caused more substantial changes in [PCr] in white muscle (Fig. 7B,D), but the effect on [ATP] was negligible in all cases. Therefore, reasonable uncertainty in the parameters that were not obtained from goldfish does not alter the conclusion that there is spatial and temporal constancy of [ATP] in both red and white fibers under the conditions simulated in our study. Likewise, uncertainty in these parameters does not alter the conclusion that spatial gradients in [PCr] (and, by extension, ΔG_{ATP}) may exist under all conditions of the simulation in activated white muscle.

Because we did not obtain a direct measurement using NMR, D_{ATP} at 5 °C was estimated on the assumption that the effects of temperature on D_{ATP} parallel the effects of temperature on D_{PCr} (Q_{10}=1.28). There is indirect evidence from studies of the thermal sensitivity of D_{ATP} in solution to support this assumption (Hubley *et al*. 1996). Furthermore, we examined the consequences of variation in D_{ATP} at 5 °C to assess whether error in this estimate could affect the results of our model. The extreme case of white muscle under the 5acc–5exp condition was analyzed, where D_{ATP}(5 °C) was calculated from D_{ATP}(25 °C) using Q_{10} values of 0, 3 and 6. Despite the 36-fold range in values of D_{ATP} at 5 °C, the resulting concentration profiles differed from one another by

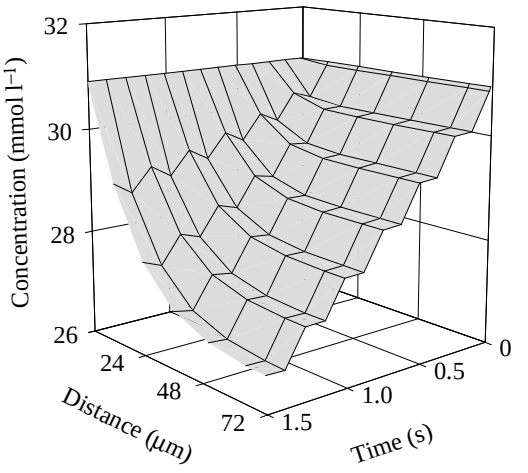

Fig. 5. Expanded profile of [PCr] in white muscle under the condition 25acc–25exp (see Fig. 4A). This figure reveals oscillations in the rate of energy utilization, which correspond to alternating contraction and relaxation during the 4 Hz tailbeat cycle.

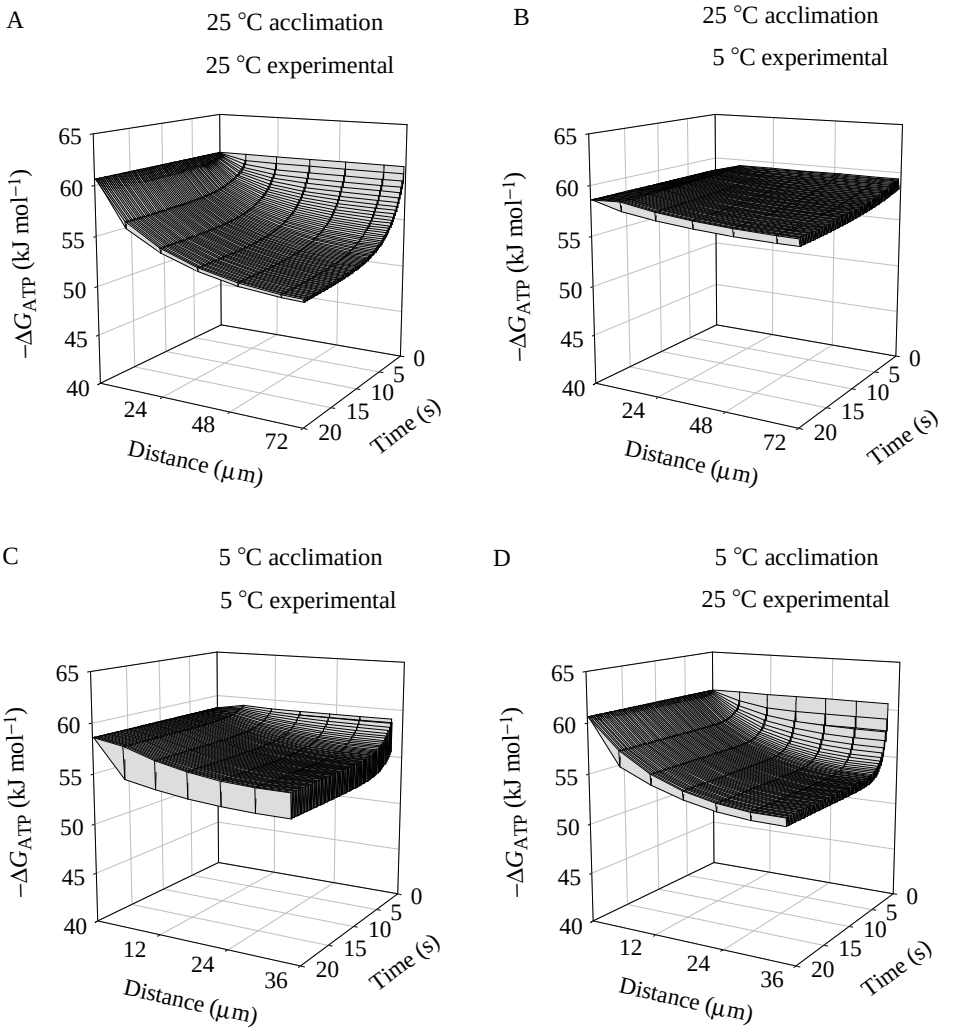

Fig. 6. Profiles of ΔG_{ATP} in activated goldfish white muscle fibers.

less than 1 %. This outcome is consistent with a predominant role for PCr diffusion in the intracellular transport of high-energy phosphate (Meyer *et al*. 1984).

The effects of acclimation-induced changes in mitochondrial density on high-energy phosphate transport can be examined by comparing Figs 2, 3, 4 and 6 with Fig. 8. Fig. 8 represents red and white muscle from goldfish under the condition 5acc*–5exp, in which the normal cold-induced proliferation of mitochondria has not occurred. In red muscle, there was little change from the normal 5acc–5exp condition. In white muscle, elimination of the increase in mitochondrial density at 5 °C resulted in greater depletion of PCr and greater reductions in $|\Delta G_{ATP}|$: after 20 s of activity under the condition 5acc*–5exp, [PCr] at $x=\lambda/2$ was reduced by 17.1 mmol l^{-1}, and $|\Delta G_{ATP}|$ at $x=\lambda/2$ was reduced by 9.4 kJ mol^{-1}. For comparison, [PCr] at $x=\lambda/2$ was reduced by 4.9 mmol l^{-1} and $|\Delta G_{ATP}|$ at $x=\lambda/2$ was reduced by 5.3 kJ mol^{-1} under the 5acc–5exp condition.

Discussion

Red muscle

The reaction–diffusion analysis of red muscle shows that intracellular [ATP], [PCr] and ΔG_{ATP} remain nearly constant throughout the muscle fibers during maximal sustained activity (Fig. 3). This outcome is readily anticipated and is consistent with the well-known ability of vertebrate oxidative muscle to resist changes in [ATP] and [PCr] during sustained activity (Driedzic and Hochachka, 1978; Kushmerick, 1985). Two notable features of highly oxidative muscle contribute to this general pattern of response. First, the relatively high volume density of mitochondria in oxidative fibers represents both a high capacity for ATP production and inherently short diffusion distances between mitochondria and other cellular compartments. Second, the low value of V_{max} for red muscle myosin ATPase, relative to that of white muscle, reflects a comparatively low demand for ATP. Temporal–spatial profiles of [ATP], [PCr] and ΔG_{ATP} in active red muscle remained nearly constant even when model conditions represented acute changes in temperature. These results indicate that an acute decrease in temperature from 25 °C to 5 °C and the accompanying reductions in D_{ATP} and D_{PCr} do not pose a significant challenge to intracellular energy transport in red fibers.

The model also permitted us to examine the impact of

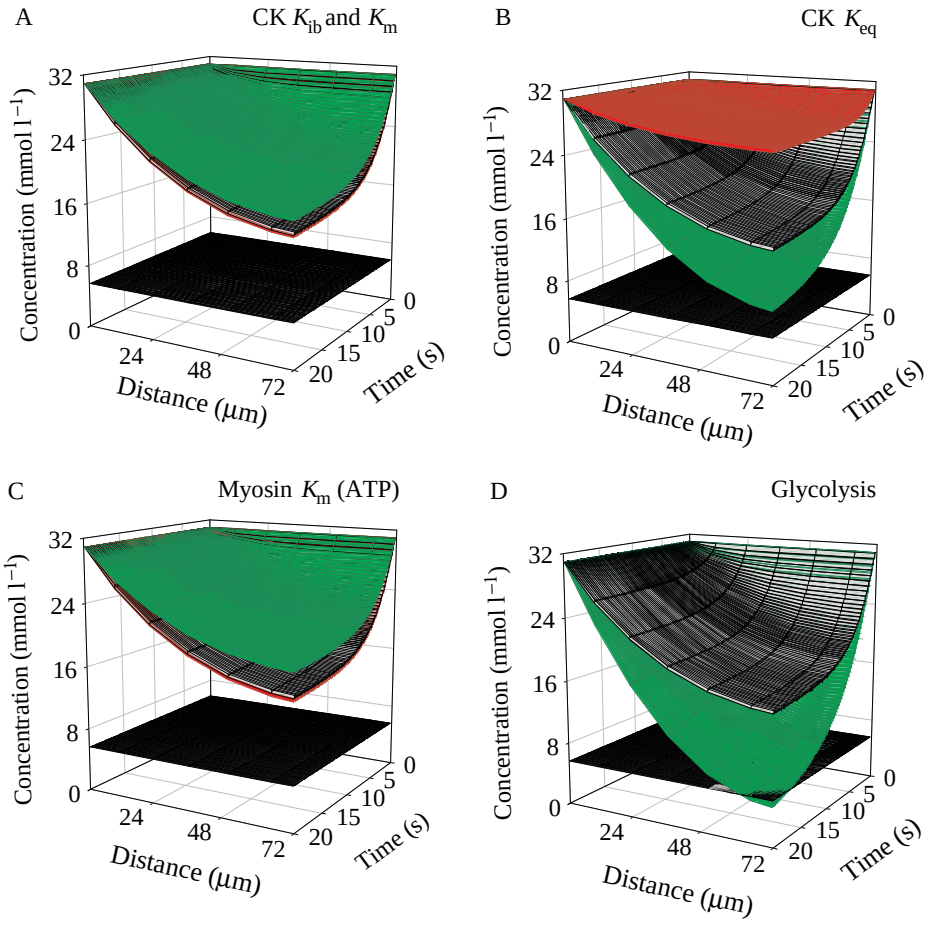

Fig. 7. Sensitivity of the model to parameters that were not obtained from goldfish. Each panel shows plots of [PCr] (upper cirves) and [ATP] (lower curves) calculated for white muscle under the condition 25acc–25exp (see Materials and methods). (A) Tenfold variation in K_{ib} for the creatine kinase (CK) reaction; changes in K_m(ADP) have the same effect as changes in K_{ib}. (B) Tenfold variation in K_{eq} for the CK reaction. (C) Tenfold variation in K_m(ATP) for myosin ATPase. (D) Removal of glycolytic ATP production. Curves shown in black are identical to those in Fig. 3A. In A–C, green represents a tenfold increase in the given parameter; red represents a tenfold decrease in the given parameter. In D, green represents the removal of glycolytic ATP production. Plots of [ATP] were very similar under all conditions.

increased mitochondrial density, which occurs during cold acclimation, on [ATP], [PCr] and ΔG_{ATP} in active red muscle. We did so by considering the 5acc–5exp condition, but with $\lambda/2$ characteristic of the 25 °C acclimation temperature (Fig. 8A,C). This situation, in which reductions in diffusion coefficients and acclimation-induced increases in myosin ATPase activity are not offset by decreased diffusion distances, should represent the most severe challenge to high-energy phosphate transport in red muscle. However, even under these conditions, there are no changes in the temporal–spatial profiles of phosphorus metabolites and ΔG_{ATP}, relative to the resting state. Thus, it appears that substantial changes in mitochondrial density and diffusion distances, which occur as a consequence of temperature acclimation, have no impact upon the capacity of red fibers to maintain constant [ATP], [PCr] and ΔG_{ATP} during contractile activity.

White muscle

Temporal–spatial profiles of [ATP] remained virtually constant in white muscle under all conditions of acclimation temperature and experimental temperature that were examined (Fig. 4), but the model shows that [PCr] and $|\Delta G_{ATP}|$ decrease markedly during 20 s of maximal activity under all conditions (Figs 4–6). These results are in good agreement with results obtained empirically in a prior study of fish white muscle (Moon *et al*. 1991). White fibers isolated from cod (*Gadus morhua* L.) were stimulated at 5 Hz, frozen after a given number of contraction cycles, and analyzed for metabolite concentrations. After 64 contraction cycles (approximately 13 s), there was no significant change in [ATP], but [PCr] had declined to 40 % of the initial value. Depletion of PCr and the concomitant change in ΔG_{ATP} in white muscle are related to the relatively low density of mitochondria, which limits oxidative ATP production, and the high demand for ATP by white muscle myosin ATPase.

Although previous biochemical analyses have amply demonstrated that activity causes a decrease in intracellular $|\Delta G_{ATP}|$ in white muscle, the reaction–diffusion model provides a significant new insight into this phenomenon: contractile activity is shown to result in the development of spatial gradients in [PCr] and ΔG_{ATP} (Figs 4–6). Fig. 5 depicts in detail the development of this gradient for [PCr], which oscillates with the alternating contraction and relaxation phases of subsequent tailbeat cycles. Similar oscillations in the gradients for ΔG_{ATP} contribute to the appearance of ‘thickness’ in the profiles shown in Fig. 6. These oscillations are superimposed on overall reductions in [PCr] and $|\Delta G_{ATP}|$ with increasing time and distance from the mitochondrial wall. The

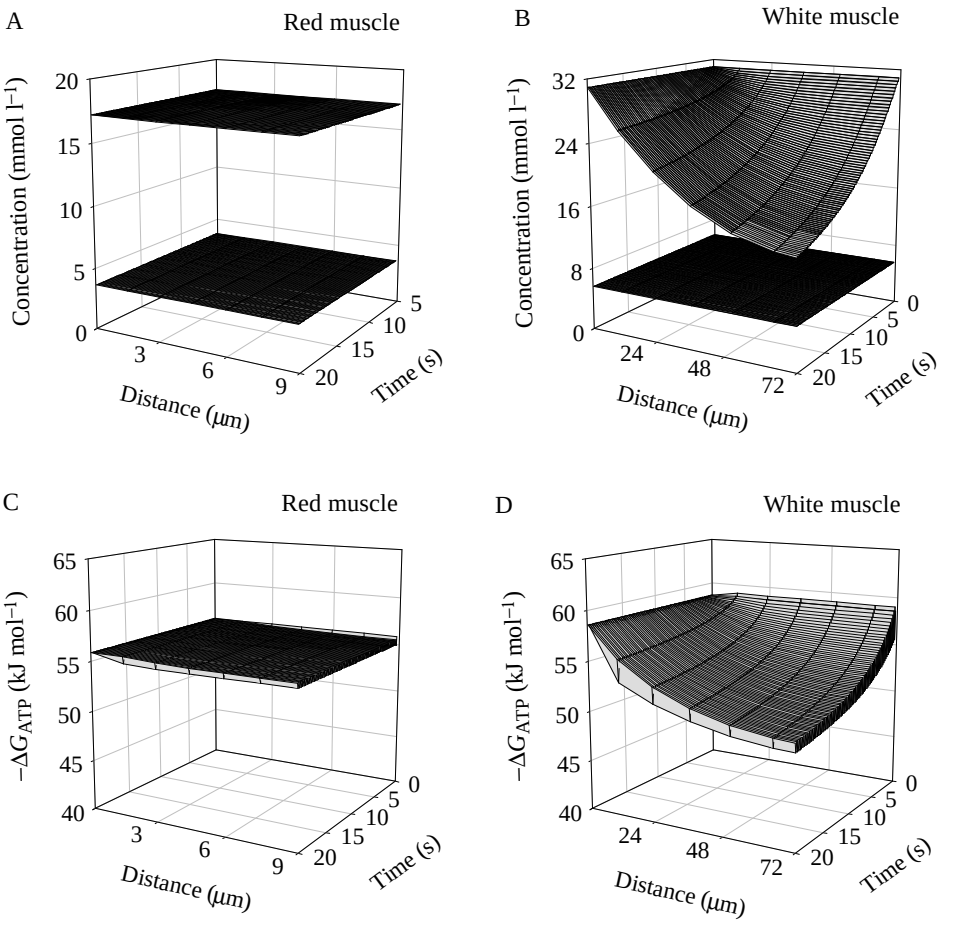

Fig. 8. The effects of changes in mitochondrial density. These profiles represent the 5acc*–5exp conditions (see Materials and methods): all profiles were calculated for 5 °C-acclimated fish at a 5 °C experimental temperature (5acc–5exp), except that mitochondrial density (and, therefore, λ/2) was that of 25 °C-acclimated goldfish. A and B show concentration profiles for red and white muscle, respectively; C and D show profiles of ΔG_{ATP} for red and white muscle, respectively.

gradients shown in Figs 4–6 should be interpreted as the upper limit of gradients *in vivo*. This is because the boundary condition $C_i=C_i^o$ at $x=0$ is equivalent to assuming that mitochondria can perfectly buffer against change in metabolite concentrations at their surface, which is unrealistic. To the extent that mitochondrial function *in vivo* is less than ideal in this regard, contractile activity of white muscle will result in less severe spatial gradients but larger global decreases in [PCr] and ΔG_{ATP}.

According to the model, the magnitudes of changes in [PCr] and ΔG_{ATP} that occur in activated white muscle depend upon both experimental and acclimation temperatures (Figs 4, 6). In general, gradients in [PCr] and ΔG_{ATP} were less severe at the 5 °C experimental temperature than at 25 °C. This result may be somewhat surprising, because the diffusion coefficients of metabolites responsible for energy transport are smaller at 5 °C than at 25 °C. The explanation for this result is that reductions in the rate of energy transport at 5 °C are offset by reductions in the demand for ATP at 5 °C. For example, the least severe gradients in [PCr] and ΔG_{ATP} in white muscle are found in 25 °C-acclimated goldfish abruptly transferred to the 5 °C experimental temperature (Figs 4B, 6B); the lowest value calculated for myosin ATPase activity in white muscle is also found in these animals (Table 2).

Acclimation to cold temperatures results in a considerable increase in myosin ATPase activity, in comparison with activity in muscle of animals abruptly transferred to cold temperatures (Johnston *et al*. 1975; Sidell, 1980; Johnson and Bennett, 1995). In the case of white muscle, the model shows a positive impact of increased mitochondrial density in offsetting this increased demand for ATP: comparison of Fig. 8 with Figs 4 and 6 shows that depletion of PCr and changes in ΔG_{ATP} are more extensive in white fibers without increased mitochondrial density (5acc*–5exp) than in normally acclimated white fibers (5acc–5exp). Therefore, the beneficial consequences of increased mitochondrial density in cold-acclimated fish may include lessening the severity of temporal–spatial gradients in [PCr] and ΔG_{ATP} and delaying the onset of fatigue during burst activity.

Whole-animal performance

The reaction–diffusion analysis shows that [ATP] remains remarkably constant in both red and white muscle under all conditions examined: neither acute changes in temperature nor acclimatory responses to changes in temperature resulted in a limitation of transport of ATP throughout the muscle fibers. However, the potential for reductions in contractile function (i.e. fatigue) during burst activity is demonstrated by changes in [PCr] and ΔG_{ATP} that occur in white muscle under all conditions of acclimation and experimental temperature. Increased concentrations of P_i, which accompany decreased [PCr], contribute directly to reductions in maximal force

generation of muscle (reviewed by Allen *et al*. 1995). Reductions in $|\Delta G_{ATP}|$ have been shown by Dawson *et al*. (1980) to be correlated with increased relaxation rates of muscle. This effect of changes in ΔG_{ATP} is attributed to diminished function of sarcoplasmic reticulum Ca^{2+}/Mg^{2+}-ATPase (Dawson *et al*. 1980; Trevorrow and Haynes, 1984), and the magnitude of this effect could be substantial: extrapolation from data for frog gastrocnemius muscle (equation 13 of Dawson *et al*. 1980) suggests that reductions in $|\Delta G_{ATP}|$ calculated for goldfish white muscle under the condition 25acc–25exp could lead to a twofold decrease in the muscle relaxation rate. Intracellular acidosis, which results from anaerobic glycolysis, is also expected to occur in white muscle, although changes in pH were not addressed explicitly in our model. The consequences of intracellular acidosis include decreases in maximal force production, myofibrillar Ca^{2+}-sensitivity, shortening velocity and myofibrillar ATPase activity (reviewed by Fitts, 1994). Thus, it is clear that changes in the concentrations of high-energy phosphate metabolites and in pH in white muscle will reduce power output during burst swimming, a locomotory regime that is powered primarily by activation of white muscle.

High-energy phosphate compounds and ΔG_{ATP} were maintained at nearly constant levels throughout red fibers at both 5 °C and 25 °C. In white fibers, high-energy phosphate compounds and ΔG_{ATP} were maintained at higher levels at 5 °C than at 25 °C. These results strongly suggest that decreased rates of intracellular high-energy phosphate transport at cold temperatures do not limit contractile function. Rather, evidence indicates that the effects of temperature on locomotory performance will be determined largely by changes in myosin ATPase activity. In a recent, *in vivo* study of goldfish burst swimming (Johnson and Bennett, 1995), the lowest maximum velocities attained during C-starts were obtained from warm-acclimated (35 °C) fish studied at a cold temperature (10 °C). In the same study, the lowest myosin ATPase activity in white fibers was also found in muscle obtained from warm-acclimated fish and assayed at the cold temperature. Similarly, the lowest sustained swimming velocities reported for carp by Rome *et al*. (1985) were obtained from warm-acclimated (26 °C) fish swimming at a cold temperature (10 °C).

In cyprinid fish (e.g. goldfish and carp), several weeks of cold-acclimation result in increased myosin ATPase activity (Johnston *et al*. 1975; Sidell, 1980; Johnson and Bennett, 1995) and improved muscle contraction kinetics (Johnston *et al*. 1985; Johnson and Bennett, 1995). Cold-acclimation also results in improved burst swimming (Johnson and Bennett, 1995) and sustained swimming (Rome *et al*. 1985) at cold temperatures. Therefore, an increased capacity to convert ATP into work is an important determinant of whole-animal locomotor performance. This relationship between temperature acclimation and the capacity to use ATP is reflected in our model by greater reductions in [PCr] and ΔG_{ATP} at 5 °C in white muscle from 5 °C-acclimated goldfish than in that from 25 °C-acclimated goldfish. This condition can be summarized as follows: the 25acc–5exp fish do not deplete their energy stores as rapidly as the 5acc–5exp fish but also do not swim as fast.

Changes in mitochondrial density

The mechanisms leading to changes in muscle ultrastructure during temperature acclimation are both important and unknown. In the present study, we found that changes in mitochondrial density in white muscle fibers may contribute to improved burst performance in cold-acclimated goldfish. Increased mitochondrial density may improve performance by offsetting the increased demand for ATP that occurs upon cold-acclimation. Our results lead us to conclude, however, that the stimulus for changes in mitochondrial volume density cannot be a disruption in intracellular energy transport *per se*. Significant changes in mitochondrial density occur with temperature acclimation in red muscle fibers, but the model shows that the putative energetic stimulus for change is absent: neither acute nor acclimatory changes in temperature have any effect on profiles of [ATP] or the free energy of ATP hydrolysis (ΔG_{ATP}) in this muscle type.

What then is the driving force behind the changes in mitochondrial density that are observed during temperature acclimation? As has been suggested previously (Johnston, 1982; Tyler and Sidell, 1984; Sidell, 1988; Egginton and Sidell, 1989), changes in mitochondrial density may compensate for changes in the rate of oxygen transport between mitochondria and capillaries. Although there is evidence that intracellular resistance to oxygen diffusion in mammalian skeletal muscle at 37 °C is minimal (Gayeski and Honig, 1986), D_{O_2} changes with a Q_{10} of 1.26 between 0 °C and 37 °C in frog sartorius muscle (Mahler *et al*. 1985). Therefore, decreases in D_{O_2} at cold temperatures may generate sufficient resistance to intracellular oxygen transport to motivate changes in mitochondrial density. It has also been suggested that the proliferation of mitochondria at cold temperatures simply offsets the reduced catalytic rates of aerobic enzymes (Johnston and Maitland, 1980; Johnston, 1982; Egginton and Sidell, 1989). A thorough analysis of the relationship between mitochondrial density and aerobic capacity may require a model that accounts directly for the effects of temperature on mitochondrial ATP production. We hope to improve upon our reaction–diffusion model by developing a model with more flexible boundary conditions, which will facilitate such an analysis.

The authors wish to thank R. Rosanske and Dr T. Gedris for assistance with NMR, M. Seavy for assistance with HPLC and Dr A. Thistle for assistance in preparation of the manuscript. This work was supported in part by NIH DK41908 to T.S.M. and a Florida State University Dissertation Fellowship to M.J.H. This work was supported in part by NIH DK41908 and a grant-in-aid from AHA (Fl affiliate) to T.S.M.

References

ALLEN, D. G., LÄNNERGREN, J. AND WESTERBLAD, H. (1995). Muscle

cell function during prolonged activity: cellular mechanisms of fatigue. *Exp. Physiol.* **80**, 497–527.

BESSMAN, S. P. AND GEIGER, P. J. (1981). Transport of energy in muscle: the phosphorylcreatine shuttle. *Science* **211**, 448–452.

BIRD, R. B., STEWART, W. E. AND LIGHTFOOT, E. N. (1960). *Transport Phenomena*. New York: Wiley.

COOKE, R. AND PATE, E. (1985). The effects of ADP and phosphate on the contraction of muscle fibers. *Biophys. J.* **48**, 789–798.

CROCKETT, E. L. AND SIDELL, B. D. (1990). Some pathways of energy metabolism are cold adapted in Antarctic fishes. *Physiol. Zool.* **63**, 472–488.

DAWSON, M. J., GADIAN, D. G. AND WILKIE, D. R. (1980). Mechanical relaxation rate and metabolism studied in fatiguing muscle by phosphorus nuclear magnetic resonance. *J. Physiol., Lond.* **299**, 465–484.

DOBSON, G. P., PARKHOUSE, W. S. AND HOCHACHKA, P. W. (1987). Regulation of anaerobic ATP-generating pathways in trout fast-twitch skeletal muscle. *Am. J. Physiol.* **253**, R186–R194.

DRIEDZIC, W. R. AND HOCHACHKA, P. W. (1978). Metabolism in fish during exercise. In *Fish Physiology* (ed. W. S. Hoar), pp. 503–543. New York: Academic Press.

EGGINTON, S. AND SIDELL, B. D. (1989). Thermal acclimation induces adaptive changes in subcellular structure of fish skeletal muscle. *Am. J. Physiol.* **256**, R1–R9.

FITTS, R. H. (1994). Cellular mechanisms of muscle fatigue. *Physiol. Rev.* **74**, 49–94.

GAYESKI, T. E. J. AND HONIG, C. R. (1986). O_2 gradients from sarcolemma to cell interior in red muscle at maximal $\dot{V}_{O_2}$. *Am. J. Physiol.* **251**, H789–H799.

HAZEL, J. R. AND PROSSER, C. L. (1974). Molecular mechanisms of temperature compensation in poikilotherms. *Physiol. Rev.* **54**, 620–677.

HUBLEY, M. J., LOCKE, B. R. AND MOERLAND, T. S. (1996). The effects of temperature, pH and magnesium on the diffusion coefficient of ATP in solutions of physiological ionic strength. *Biochim. biophys. Acta* **1291**, 115–121.

HUBLEY, M. J. AND MOERLAND, T. S. (1995). Application of homonuclear decoupling to measures of diffusion in biological ^{31}P spin echo spectra. *NMR Biomed.* **8**, 113–117.

HUBLEY, M. J., ROSANSKE, R. C. AND MOERLAND, T. S. (1995). Diffusion coefficients of ATP and creatine phosphate in isolated muscle: pulsed gradient ^{31}P NMR of small biological samples. *NMR Biomed.* **8**, 72–78.

JAYNE, B. C. AND LAUDER, G. V. (1993). Red and white muscle activity and kinematics of the escape response of the bluegill sunfish during swimming. *J. comp. Physiol.* A **173**, 495–508.

JAYNE, B. C. AND LAUDER, G. V. (1995). Red muscle motor patterns during steady swimming in largemouth bass: effects of speed and correlations with axial kinematics. *J. exp. Biol.* **198**, 1575–1587.

JOHNSON, T. P. AND BENNETT, A. F. (1995). The thermal acclimation of burst escape performance in fish: an integrated study of molecular and cellular physiology and organismal performance. *J. exp. Biol.* **198**, 2165–2175.

JOHNSTON, I. A. (1979). Calcium regulatory proteins and temperature acclimation of actomyosin ATPase from a eurythermal teleost (*Carassius auratus* L.). *J. comp. Physiol.* **129**, 163–167.

JOHNSTON, I. A. (1982). Capillarisation, oxygen diffusion distances and mitochondrial content of carp muscles following acclimation to summer and winter temperatures. *Cell Tissue Res.* **222**, 325–337.

JOHNSTON, I. A., DAVISON, W. AND GOLDSPINK, G. (1975). Adaptations in Mg^{2+}-activated myofibrillar ATPase activity induced by temperature acclimation. *FEBS Lett.* **50**, 293–295.

JOHNSTON, I. A. AND LUCKING, M. (1978). Temperature induced variation in the distribution of different types of muscle fibre in the goldfish (*Carassius auratus*). *J. comp. Physiol.* **124**, 111–116.

JOHNSTON, I. A. AND MAITLAND, B. (1980). Temperature acclimation in crucian carp, *Carassius carassius* L., morphometric analyses of muscle fibre ultrastructure. *J. Fish Biol.* **17**, 113–125.

JOHNSTON, I. A., SIDELL, B. D. AND DRIEDZIC, W. R. (1985). Force–velocity characteristics and metabolism of carp muscle fibres following temperature acclimation. *J. exp. Biol.* **119**, 239–249.

KRAB, K. AND VAN WEZEL, J. (1992). Improved derivation of phosphate potentials at different temperatures. *Biochim. biophys. Acta* **1098**, 172–176.

KUSHMERICK, M. J. (1985). Patterns in mammalian muscle energetics. *J. exp. Biol.* **115**, 165–177.

LANGFELD, K. S., CROCKFORD, T. AND JOHNSTON, I. A. (1991). Temperature acclimation in the common carp: force–velocity characteristics and myosin subunit composition of slow muscle fibres. *J. exp. Biol.* **155**, 291–304.

LOWRY, O. H. AND PASSONNEAU, J. V. (1972). *A Flexible System of Enzymatic Analysis*. New York: Academic Press.

MAHLER, M., LOUY, C., HOMSHER, E. AND PESKOFF, A. (1985). Reappraisal of diffusion, solubility and consumption of oxygen in frog skeletal muscle, with applications to muscle energy balance. *J. gen. Physiol.* **86**, 105–134.

MEYER, R. A., SWEENEY, H. L. AND KUSHMERICK, M. J. (1984). A simple analysis of the 'phosphocreatine shuttle'. *Am. J. Physiol.* **246**, C365–C377.

MOERLAND, T. S. (1995). Temperature: enzyme and organelle. In *Biochemistry and Molecular Biology of Fishes* (ed. P. W. Hochachka and T. P. Mommsen), pp. 57–71. Amsterdam: Elsevier.

MOON, T. W., ALTRINGHAM, J. D. AND JOHNSTON, I. A. (1991). Energetics and power output of isolated fish fast muscle fibers performing oscillatory work. *J. exp. Biol.* **158**, 261–273.

PATE, E. AND COOKE, R. (1985). The inhibition of muscle contraction by adenosine 5′ (β, γ-imido) triphosphate and by pyrophosphate. *Biophys. J.* **47**, 773–780.

ROME, L. C., LOUGHNA, P. T. AND GOLDSPINK, G. (1984). Muscle fiber activity in carp as a function of swimming speed and muscle temperature. *Am. J. Physiol.* **247**, R272–R279.

ROME, L. C., LOUGHNA, P. T. AND GOLDSPINK, G. (1985). Temperature acclimation: improved swimming performance in carp at low temperatures. *Science* **228**, 194–196.

SCHIMERLIK, M. I. AND CLELAND, W. W. (1973). Inhibition of creatine kinase by chromium nucleotides. *J. biol. Chem.* **248**, 8418–8423.

SEGEL, I. H. (1993). *Enzyme Kinetics*. New York: Wiley.

SIDELL, B. D. (1980). Responses of goldfish (*Carassius auratus*, L.) muscle to acclimation temperature: alterations in biochemistry and proportions of different fiber types. *Physiol. Zool.* **53**, 98–107.

SIDELL, B. D. (1988). Diffusion and ultrastructural adaptive responses in ectotherms. In *Microcompartmentation* (ed. D. P. Jones), pp. 71–92. Boca Raton, FL: CRC Press.

SIDELL, B. D. AND HAZEL, J. R. (1987). Temperature affects the diffusion of small molecules through cytosol of fish muscle. *J. exp. Biol.* **129**, 191–203.

SIDELL, B. D. AND MOERLAND, T. S. (1989). Effects of temperature on muscular function and locomotory performance in teleost fish. In *Advances in Comparative and Environmental Physiology* (ed. C. P. Mangum and R. Gilles), pp. 115–156. Berlin: Springer-Verlag.

TEAGUE, W. E. AND DOBSON, G. P. (1992). Effect of temperature on the creatine kinase equilibrium. *J. biol. Chem.* **267**, 14084–14093.

TREVORROW, K. AND HAYNES, D. H. (1984). The thermodynamic efficiency of the Ca^{2+}-Mg^{2+}ATPase is one hundred percent. *J. Bioenerg. Biomembr.* **16**, 53–59.

TYLER, S. AND SIDELL, B. D. (1984). Changes in mitochondrial distribution and diffusion distances in muscle of goldfish upon acclimation to warm and cold temperatures. *J. exp. Zool.* **232**, 1–9.

VAN DEN THILLART, G., VAN WAARDE, A., MULLER, H. J., ERKELENS, C. AND LUGTENBURG, J. (1990). Determination of high-energy phosphate compounds in fish muscle, ^{31}P-NMR spectroscopy and enzymatic methods. *Comp. Biochem. Physiol.* **95**B, 789–795.

VAN WAARDE, A., VAN DEN THILLART, G., ERKELENS, C., ADDINK, A. AND LUGTENBURG, J. (1990). Functional coupling of glycolysis and phosphocreatine utilization in anoxic fish muscle. *J. biol. Chem.* **265**, 914–923.

WALESBY, N. J. AND JOHNSTON, I. A. (1980). Temperature acclimation in brook trout muscle: adenine nucleotide concentrations, phosphorylation state and adenylate energy charge. *J. comp. Physiol.* **139**, 127–133.

WATTS, D. C. (1973). Creatine kinase (adenosine 5′-triphosphate-creatine phosphotransferase). In *The Enzymes* (ed. P. D. Boyer), pp. 383–455. New York: Academic Press.

WISEMAN, R. W., MOERLAND, T. S., CHASE, P. B., STUPPARD, R. AND KUSHMERICK, M. J. (1992). High-performance liquid chromatographic assays for free and phosphorylated derivatives of the creatine analogues β-guanidopropionic acid and 1-carboxymethyl-2-iminoimidazolidine (cyclocreatine). *Analyt. Biochem.* **204**, 383–389.